Numerical computation of seepage erosion below dams (piping)

J.B. Sellmeijer
GeoDelft, Delft, The Netherlands

I. Introduction

In delta areas the land is protected from floods and high tides by dikes. In general these are constructed of impervious clays and built on a sandy aquifer as subsoil. Such structures are vulnerable to an erosion effect called piping.

The actual word 'piping' refers to the development of shallow channels in the sand below the dike, which begins at the downstream side of the structure. Here often a ditch is situated with a burst bottom due to excess water pressures. The subsequent erosion process develops backwards to the high head side. The natural non-homogeneity in the soil causes the shallow channels to be irregularly shaped.

Below a critical value of the hydraulic head over the structure the erosion process eases down until water only is transported through the channels. It is common to observe sand boils behind the dike, which produce water alone. However, if a critical head difference is reached, the erosion process continues and the structure may in the end collapse.

II. Historical Notes

During the beginning of the previous century the piping phenomenon has been intensively studied. References [1] through [5] show in its perspective the way piping was considered and understood. Simple empirical rules for the critical gradient were applied with some theoretical backup.

TABLE I.
SOME EXAMPLES OF SIMPLE PIPING RULES

Bligh $\frac{H}{L} = \frac{1}{C_{\text{Bligh}}}$	fine silty sand moderate fine sand course sand fine gravel course gravel		C_{Bligh} 18 15 12 9 4
Lane $\frac{H}{L_h} = \frac{\frac{1}{3}+\frac{L_v}{L_h}}{C_{\text{Lane}}}$	fine silty sand moderate fine sand course sand fine gravel course gravel		C_{Lane} 8.5 7 5 4 3
Sellmeijer $\frac{H}{L} = GRSF$	geometry factor rolling equilibrium sand properties 4 force factor	$G = \left(\frac{D}{L}\right)^{\frac{0.28}{\left(\frac{D}{L}\right)^{2.8}-1}}$ $R = \frac{g'_p}{g_w}\tan J$ $S = h\frac{d}{\sqrt[3]{k\,L}}$ $F = 0.68 - 0.1\ln(S)$	D: aquifer height H: hydraulic head L: dike width g_p: unit weight particles g_w: unit weight water J: bedding angle h: Whites constant d: particle diameter k: intrinsic permeability

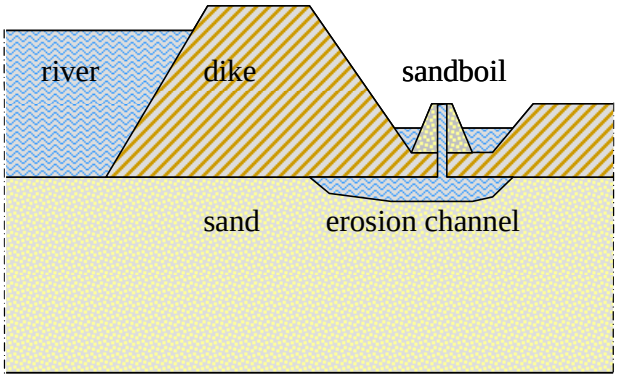

Figure 1. Geometry of the standard dike

In the second half of the previous century extended programs of visual tests were carried out. Based on these observations numerical models were developed. References [6] through [16] represent the activities during this period.

The simple piping rules for the critical gradient are meant for ordinary consultancy. These rules are easy to handle and provide results instantaneously. They are applicable to a standard dike, shown in Figure 1. The sand is considered to be homogeneous and the geometry consists of a horizontal layer with a clay dike on top. Note that the dimensions of the erosion channel and sand boil are exaggerated in order to view them properly.

Examples of the simple rules are collected in Table I. The first two are empirical. They specify the role of the soil properties by a characteristic factor. This factor is read from a table after classification of the sandy material.

The third rule is obtained by calculation by a conceptual model. A number of specific results is curve fitted and collected into the rule. This has the advantage that the soil properties are involved by their parameter values. These values may be measured or determined by correlation.

III. Advanced Numerical Piping Modelling

The simple piping rules are fine for standard consultancy. However, they are insufficient for complicated problems, where risks are high. Then, a more refined approach is required.

For instance, the rules do not consider the effect of a course gravel sublayer below the sandy layer. Nor a sloping bottom of the dike, the role of a partially covered river bottom by slurry, the effect of varying layer thickness, etc. .

For these cases a versatile numerical tool is required. Such a model is described in reference [12]. In fact it is used for the derivation of the third simplified piping rule. The groundwater flow, here, was modeled by the analytical technique of conformal mapping. For simple geometries this is possible.

For more complex geometries an analytical approach is no longer feasible. A numerical model will be presented.

A. *Numerical piping program*

The conceptual piping model consists of three areas: the groundwater flow in the layers, the water flow in the erosion channel and the state of limit equilibrium of the particles at the bottom of the channel.

The last two areas together form the boundary condition for the first area. That means that the problem of piping may be determined by ordinary groundwater flow computation with a special piping boundary condition.

However, this is a cumbersome condition. It is highly non linear. It is not operative in a single point of the boundary, but affects the boundary on aggregate. By implication, only iteratively this condition may be applied.

B. *Condition of continuity in the erosion channel*

The erosion channel appears to be very shallow. This is observed in the visual tests; see [8], [10], [11], [14], [15]. Results by computation also show extremely shallow channels; see [12]. Apparently, quite a lot of seepage water may flow off through a small open channel.

The flow in the channel may be modeled by the laminar Navier Stokes equations. For a sandy sublayer the flow is laminar; for course gravel it might tend to become turbulent. Since the channel is so shallow, the solution of the Navier Stokes equations is not unlike the formula for pipe flow. It reads:

$$a^3 p = 12\, k\, \frac{Q}{k}. \qquad (1)$$

a is the height of the channel; p is the gradient in the channel; Q is the discharge in the channel; k is the intrinsic permeability and k the hydraulic permeability. The hydraulic and intrinsic permeabilities are linked by the viscosity.

The solution supplies also the shear stress along the bottom of the channel. This stress is caused by the momentum of the flow through the channel. It reads:

$$t = \tfrac{1}{2} g_w\, p\, a. \qquad (2)$$

This stress is required to determine the limit stress state of the particles.

C. *Limit stress state of the bottom particles*

The question of limiting stability at the interface of soil and water cannot be solved by regarding the soil as a continuum. This is due to the fact that continuum mechanics allow the effective vertical stresses to vanish near the bottom of the slit. The shearing stress which is associated with the near parabolic velocity profile in the slit itself, therefore, cannot be dealt with then in a Coulomb manner.

Conversely, the condition of limiting equilibrium must be imposed to the balance of forces on a particle. This yields a connection for the forces for a given mode of motion. Two modes of motion are feasible: translation and rolling. Koenders [17] showed that the rolling mode is preferred. The result is a rule not unlike a Coulomb criterion.

In the original work of [12] four distinct forces are considered for the force balance for a grain at the top of the interface. The horizontal ones are the drag force due to channel flow and the horizontal seepage gradient. The vertical ones are the weight of a particle and a force associated with the vertical seepage gradient.

However, heterogeneous mixture in steady state shows a landscape where the large grains stick out and the small ones are well buried. Between the large grains substantial open space occurs. The forces due to the seepage gradients by no means can affect the grain at the top of the interface.

By implication, two forces should be balanced, see **Figure 2**. The force along the sloping channel is the shear stress (2) times the equivalent area d^2 / h. White's constant h takes care of the substantial open space between the top grains. The vertical force is the weight of a spherical particle. The rolling mode balance of these two forces follows from the sine law in geometry:

$$\frac{g'_p \frac{p}{6} d^3}{\cos J} = \frac{\frac{1}{2} g_w\, p\, a\, d^2}{\sin(J + a)\, h}. \qquad (3)$$

a is the slope of the erosion channel.

D. *Boundary condition along the erosion channel*

An appropriate expression for the boundary condition along the erosion channel follows from (1) and (3). If the yet unknown height of the channel is eliminated, an expression remains with flow features only. It reads:

$$\sqrt[3]{\frac{Q}{k\, L}\, p^2} = \frac{p}{3} h\, \frac{g'_p}{g_w}\, \frac{\sin(J + a)}{\cos J}\, \frac{d}{\sqrt[3]{12\, k\, L}}. \qquad (4)$$

This is a suitable boundary condition for the flow. It relates the discharge on aggregate to the gradient. The

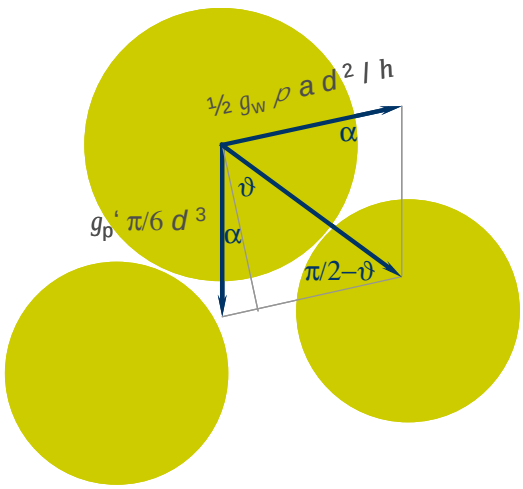

Figure 2. Two force balance of a top grain

right hand side is a constant. The erosion channel needs not to be straight. It may consist of several parts with different angles a .

E. Groundwater flow computation

It appeared that piping may be described as boundary condition in a groundwater flow program. That does not imply that such a program may be run to make predictions for piping design. Since the condition is non linear and is applied on aggregate over the boundary, a special iteration module is required.

Therefore, a shell is developed in order to control the iteration. If needed, the groundwater flow computation is called, where the current head or discharge in the piping boundary is applied. The shell examines how accurate the piping condition is met and adjusts the current head or discharge.

The head or discharge along the boundary is simulated by a number of shape functions. A few shape functions is sufficient, since the gradient is rather smooth. At the inflow point the gradient buckles, since the discharge tends to zero.

Despite the smooth character of the gradient the iteration process is a struggle. The reason is not the buckle at the inflow point. It is the fact that a change of the discharge easily compensates the one of the gradient without apparent improvement of the accuracy, see left hand side of (4).

A useful remedy for this problem is to pin down the incremental expression for the discharge at the inflow point. This expression reads:

$$\Delta Q_{\mathrm{j}} = \sum \frac{\partial Q_{\mathrm{j}}}{\partial S_{\mathrm{i}}} \Delta S_{\mathrm{i}} + \frac{\partial Q_{\mathrm{j}}}{\partial H} \Delta H \cdot \qquad (5)$$

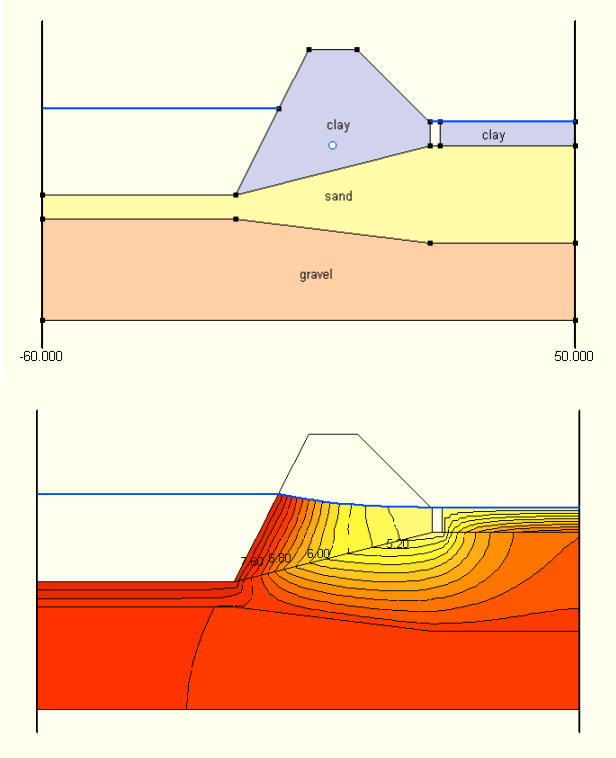

Figure 3. Example advanced piping design

S is the strength of the shape functions. The derivatives of the discharge are delivered by the groundwater flow program. Often the groundwater flow is linear, so that the incremental notation may be omitted. In the inflow point the discharge theoretically vanishes. However, since the gradient buckles, it is better to apply a small positive value, which is fixed by minimizing the inaccuracy.

Pinning down the discharge at the inflow point introduces some inaccuracy so as to make the process stable and fast. Since the outcome is calibrated by precise large scale testing results, this is justified.

An example of advanced piping design is presented. In **Figure 3** the geometry is shown at the top. The dike is sloping and situated on a two-layer subsoil. It slopes upwards, which reduces the danger for piping, since particles must roll upwards. The opposite would endanger the piping thread and should be avoided.

The upper layer is sand and the lower one gravel. The presence of the very permeable gravel endangers the piping thread. The river water flows directly downwards through the thin sand layer to the gravel. At a minimum of head loss it flows though the gravel until down under the outflow point. There it flows upwards to the erosion channel. In this way more water reaches the channel than in the case of sand alone.

In **Figure 4** the effect of the gravel is illustrated. In the top picture the gravel has the same permeability as the sand. The critical hydraulic head appears to be 4.4 m. In the bottom picture the gravel is 100 times more permeable than the sand. The critical hydraulic head appears to be 2.7 m. In the bottom picture of **Figure 3** the contour lines of the head are shown for the permeable gravel. The minimum head loss is clearly observed.

The left side of the curves in **Figure 4** represents the safe and steady state of the piping phenomenon. A small

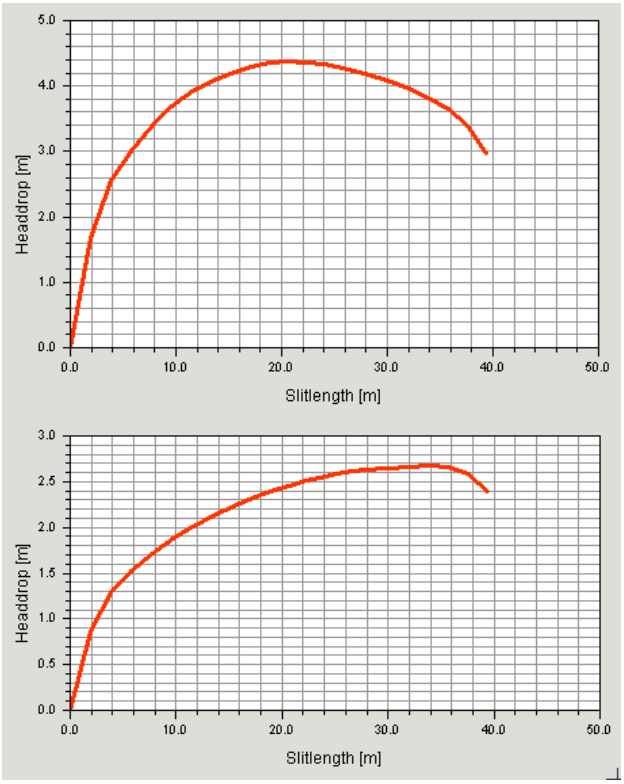

Figure 4. Output advanced piping design

disturbance is compensated by a small increase of the channel length. However, in the right side this would lead to progressive erosion. The maximum of the curves is associated with the critical head.

IV. PIPING NEURAL NETWERK

Numerical piping computations last between dozens of seconds to a dozen of minutes. If the goal of piping design is probabilistic of nature, this takes too long. A computation requires ample preparation, while consultancy prefers ready made approaches. Therefore, acceleration is sought in the design process.

The answer is the development of a new advanced piping rule, like the third one in Table I. An appropriate means to facilitate this is the use of an Artificial Neural Network. Neural networks are meant for pattern recognition, [18]. The pattern to be recognized could be a handwriting, fingerprint, but also results of piping computations. The advantage is that results of laborious computation are available at snapping one's fingers.

To set up a proper network the degrees of freedom must be limited as much as possible. Every freedom multiplies the required number of data by a factor depending on its complexity. Therefore, the piping parameters are first grouped together into meaningful clusters.

A single piping computation determines the critical head as function of the geometry and soil parameters. The Result, however, may be interpreted as the critical width of the dike as function of the head over the dike and geometry and soil parameters. Therefore, two useful types of neural networks may be derived: one for the classification of the critical head and one for the critical width of the dike.

Engineers prefer the last one, since the head occurs according to river discharge and the width of the dike may be designed.

A. Clustering parameters in the piping model

The aim is to obtain a network for a geometry with a sloping dike and two sublayers, shown in **Figure 5**. The layer heights are denoted by h with a two letter index. 'g' indicates 'granular' and 's' 'sublayer'; 1 refers to river side and 2 to polder side.

Two important scaling operations are possible: for the geometry and for the outcome. On one hand the geometry

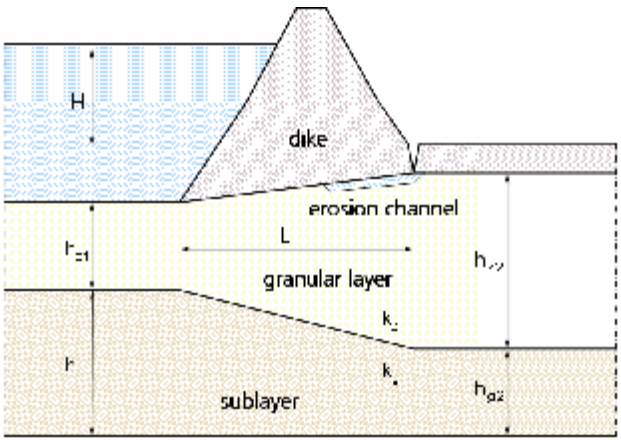

Figure 5. Geometry for the neutral network

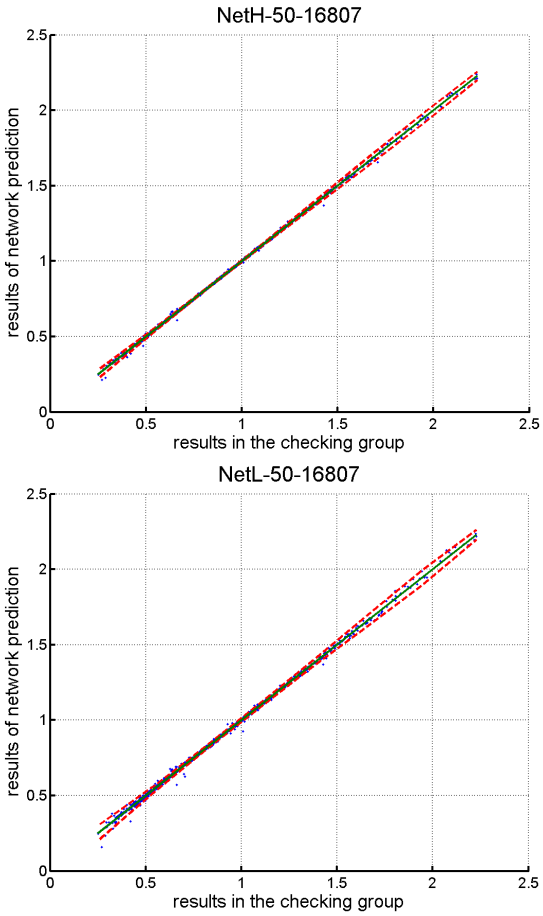

Figure 6. Neural network accuracy

may be scaled by the width of the dike, when the critical head is sought. On the other hand it may be scaled by the hydraulic head, when the critical width of the dike is sought.

The outcome (the critical head or the critical width of the dike) may be scaled by the right side of (4). It contains the width of the dike, which is better replaced by one of the neutral heights of the layers.

Thus, the general solution is specified in the following fashion:

$$\frac{1}{b}\frac{H}{L} = \mathrm{F}\left(\frac{h_{z1}}{L}, \frac{h_{z2}}{L}, \frac{h_{g1}}{L}, \frac{h_{g2}}{L}, \frac{k_z}{k_g}\right). \qquad (6)$$
$$b\,\frac{L}{H} = \mathrm{G}\left(\frac{h_{z1}}{H}, \frac{h_{z2}}{H}, \frac{h_{g1}}{H}, \frac{h_{g2}}{H}, \frac{k_z}{k_g}\right)$$

where,

$$b = \frac{p}{3} h \frac{g'_p}{g_w} \frac{\sin(J+a)}{\cos J} \frac{d}{\sqrt[3]{k\, h_{z2}}}. \qquad (7)$$

The factor b is a multiplier and need not to be incorporated in the neural network. Both networks have 5 degrees of freedom, 4 heights and the permeability contrast of the layers.

B. *Network training*

A neural network consists of layers of nodes. There are three types: input layer, hidden layers, output layer. The data in every node of a layer are passed by weight factors to all nodes of the next layer. In the nodes the data are transformed. The input nodes are filled with input. The output node(s) contain(s) the outcome. The number of hidden layers may be more than one, but this does not necessarily improve the result.

The number of hidden nodes affects the behavior of the network. Few nodes have a smoothing effect on irregularities. However, the result will be inferior for an abrupt course of the outcome. Many nodes facilitate a precise pattern recognition without too much smoothing. Here, 5 input nodes, 50 hidden nodes and 1 output node are applied.

Both networks are trained by the results of in total 18674 piping computations. 90% (16807) is used for the training, the remaining ones are applied for checking. The accuracy is shown in **Figure 6**.

Here, the input value is plotted against the result of network prediction. For a perfect fit a line under 45° would be found. The dotted lines represent the standard deviation of the difference. The top picture reflects the network for the critical head; the bottom picture for the critical width of the dike.

The agreement is rather good. The differences are very small, as may be expected for well performed computations. In some corners of the parameter space the behavior is more abrupt of nature, resulting occasionally in a minor hop.

The training data cover only that part of the parameter space, where computations are carried out. The network is applicable in that area alone. Beyond, preposterous predictions would be obtained, which are of no use and should be avoided.

C. *Advanced piping rule applied to standard dike*

The accuracy of the network prediction looks promising according to the results for the checking group in **Figure 6**.

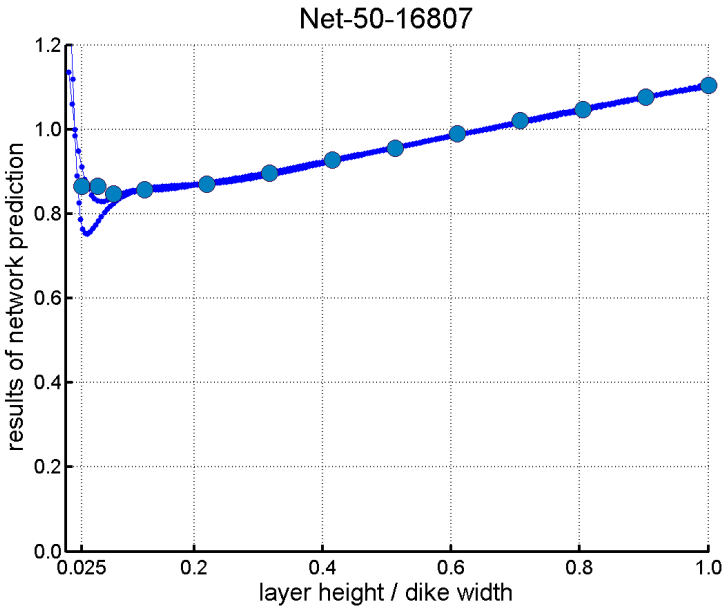

Figure 7. Advanced piping rule applied to standard dike

However, the few incidental hops are a source of concern. Therefore, it makes sense to observe the behavior in a specific range. A suitable range is the geometry of the standard dike.

Figure 7 shows the predictions by both networks (solid lines). The ones for the critical height are directly determined for the ratio of layer height and dike width. The ones for the critical dike width are determined for the ratio of layer height and hydraulic head. They are presented in the same fashion as the critical height.

For reference, the outcome of individual computations is added as large dots. In the range $h_{g2} / L > 0.1$ the agreement is excellent. For thin layers there appears to be a complication.

The problem is that the finite element groundwater flow calculation requires a few elements over the layer height in order to facilitate accurate computation. For thin layers this is not possible anymore. Very thin layers have one element only, often distorted.

No computations in the range $h_{g2} / L < 0.025$ have been made. Therefore, in that area no predictions are possible. Due to poor computation results for the smaller layer heights the predictions in the area $0.025 < h_{g2} / L < 0.1$ are less accurate.

The predictions by the neural networks still must be multiplied by the factor b in (7). For thin granular layers this factor is high, so that the risk for piping is small. However, accurate calculations must be possible also for thin layers.

V. Conclusion and Summary

For the design against piping, simple rules are used to specify the critical gradient over the dike. These rules apply to a standard dike. They do not facilitate advanced calculations.

The mechanism of piping is embodied into a conceptual model. This model is incorporated into a numerical program. By this program advanced piping computations may be carried out.

For an advanced geometry consisting of two granular layers with a sloping dike on top, a large amount of random computations is carried out. Neural networks are trained by the results of these computations. The networks in fact are a new advanced piping rule. There is a network for prediction of the critical head and one for the critical width of the dike.

The performance of the neural networks is excellent, as long as proper numerical computations are available. At present the granular height is by the dike width, the subsoil height by half the dike width.

For very thin granular layers the computations are not yet accurate enough. By implication, the networks must be used with care. The first priority is to assure detailed accuracy of the numerical flow calculation for the entire range of engineering practice, especially for very thin layers.

VI. UNITS

D	[m]	:	aquifer height
H	[m]	:	hydraulic head
L	[m]	:	dike width
Q	[m^2/s]	:	erosion channel discharge
a	[m]	:	erosion channel height
d	[m]	:	particle diameter
h	[m]	:	layer height
k	[m/s]	:	hydraulic permeability
p	[-]	:	erosion channel gradient
γ_p	[kN/m^3]	:	unit weight particles
γ_w	[kN/m^3]	:	unit weight water
a	[DEG]	:	erosion channel angle
J	[DEG]	:	bedding angle
h	[-]	:	Whites coefficient
k	[m^2]	:	intrinsic permeability

REFERENCES

[1] J. Clibborn and J.S. Beresford, "Experiments on the Passage of Water through Sand", *Govt. of India, Central Printing Office*, 1902.

[2] W.G. Bligh, "Dams Barrages and Weirs on Porous Foundations", *Engineering News*, p. 708, 1910.

[3] W.M. Griffith, "The Stability of Weir Foundations on Sand and Soil Subject to Hydrostatic Pressure", *Minutes of Proceedings J.C.E.* , Vol. 197 pt III, p. 221, 1913.

[4] L.F. Harza, "Uplift and Seepage under Dams on Sand", *Proceedings ASCE*, Paper no. 1920, 1935.

[5] E.W. Lane, "Security from Under-Seepage Masonry Dams on Earth Foundations", *Transactions ASCE*, Vol. 100 , Paper no. 1919, 1935.

[6] D. Miesel, "Rückschreitende Erosion unter Bindiger Deckschicht", Vorträge der Baugrundtagung, Berlin, *Deutsche Gesellschaft für Erd- und Grundbau E. V.*, 1978.

[7] H. Müller-Kirchenbauer, "Zum Zeitlichen Verlauf der Rückschreitenden Erosion in Geschichtetem Untergrund unter Dämmen und Stauanlagen", *Beitrag zum Talsperrensymposium*, München, 1978.

[8] J.M. de Wit, J.B. Sellmeijer, A. Penning, "Laboratory Testing on Piping", *Proceedings of the 10th International Conference on Soil Mechanics and Foundation Engineering*, Stockholm, Part 1 , p. 517, 1981.

[9] D. Van Zyl, and M.E.Harr, "Seepage Erosion Analysis of Structures", *Proceedings of the Tenth International Conference on Soil Mechanics and Foundation Engineering*, Stockholm, Part 1, p. 503, 1981.

[10] U. Hanses, H. Müller-Kirchenbauer, S. Stavros, "Zur Mechanik der Rückschreitenden Erosion unter Deichen und Dämmen", *Bautechnik 5*, pp. 163-168, 1985.

[11] I. Kohno, M. Nishigaki, Y. Takeshita, "Levee failure caused by seepage and preventive measures", *Natural Disaster Science*, V. 9, No. 2, pp 55-76, 1987.

[12] J.B. Sellmeijer, "On the Mechanism of Piping under Impervious Structures (Thesis)", *LGM-Mededelingen*, No. 96, October 1988.

[13] J.B. Sellmeijer, E.O.F. Calle, J.W. Sip, "Influence of Aquifer Thickness on Piping below Dikes and Dams", *Proc. CIGB ICOLD*, Copenhagen, July 1989, pp. 357 – 366.

[14] J.B.A. Weijers and J.B. Sellmeijer, "A new model to deal with the piping mechanism", *Filters in Geotechnical and Hydraulic Engineering*, Brauns, Heibaum & Schuler (eds), © 1993 Balkema, Rotterdam, ISBN 90 5410 342 6, 1993.

[15] J.H. Schmertmann, "The no-filter factor of safety against piping through sands", *ASCE special volume*, 2000.

[16] Xing Zheng Wu, "Probabilistic Risk Analysis and Safety Evaluation of Dikes", *Research Centre of Flood and Drought Disaster of the Ministry of Water Resources in China (RCDR) China Institute of Water Resources and Hydropower Research (IWHR)*, 2003.

[17] M. A. Koenders, "Hydraulic Criteria for Protective Filters", *private communication*, 1987.

[18] C.M. Bishop, "Neural Networks for Pattern Recognition", *Oxford University Press*, ISBN 019853864, 1995.